InP/InGaAs Uni-Traveling-Carrier Photodiode (UTC-PD) with Improved EM Field Response

Maria Jabeen, Shyqyri Haxha*, *Senior Member IEEE,* Ian Flint, Turgut Öztürk, Martin Charlton and Fathi AbdelMalek

***Abstract*— In this paper a unique structure of InP/InGaAs Uni-Traveling-Carrier Photodiode (UTC-PD) is proposed. Compared with the one-sided junction photodiode, the UTC-PD has the advantages of simpler epitaxial layer structure while maintaining the characteristics of high bandwidth and high output power loss profile. Simulated results show that a large built-in electric field can be generated under illumination which aids UTC carrier velocity. The merits of the new structure are compared to a standard UTC-PD photodiode in terms of improved electric field and carrier concentration response. It is demonstrated that the photogeneration and light absorption of UTC-PD's is improved by incorporating a step-like internal texture of cones and dots profile in the photo absorption layer. The simulated device shows a peak electrical 3-dB bandwidth of 65 GHz at a low light intensity and reverse bias voltage. The performance characteristics of 1D and 2D UTC-PD simulations including internal electric field distribution, energy band diagram, carrier concentration, and power loss distribution, are carefully studied. A theoretical discussion of the working principal and key performance characteristics of a UTC-PD enhanced by heterojunction design are reported. The entire physical environment is modelled and simulated through Finite Element Method (FEM) using commercial software. The proposed photodiode structure configuration is designed and optimised for photodetectors for high RF frequencies at different light intensities. To our knowledge, the obtained bandwidth and electric field response is the fastest among those reported for other various higher wavelength photodiodes.**

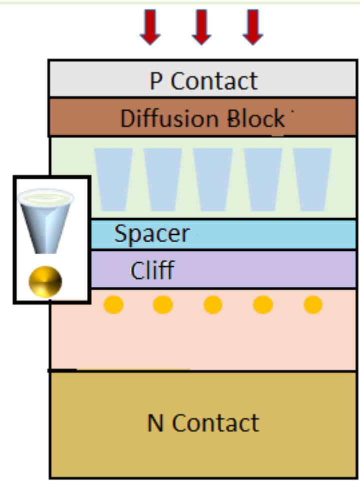

***Index Terms*—Uni-traveling Carrier Photodiode, Nano cones, InGaAs, InP, high EM distribution, extreme Electric field, Carrier velocity**

I. Introduction

PHOTODIODES are vital photonic components for many applications, including sensing, radio-over fibre wireless communications methods, high-speed fibre optic systems, and terahertz or millimetre wave generation stratagems etc [1], [2]. A photodiode can possibly operate more quickly than a transistor but on its own it cannot offer electrical amplification unlike a transistor. In 1997, a new design of photodiode was established; namely the Uni-Traveling-Carrier Photodiode (UTC-PD). The UTC-PD works at much faster modulations and with better linearity. This was achieved by removing the low hole mobility as the rate limiting factor [3]. Practical measurements of the UTC PD confirmed UTC as beneficial to PD operation [4]. Even with the improvements of the UTC photodiodes are a significant constraint in the performance of photonic systems, therefore there is an urgent need to develop higher speed and higher output power photodiodes [3], [4].

Conventional P-I-N Photodiodes (PIN-PD) were used before the invention of UTC-PD; have wide bandwidths – typically up to a 100 GHz [5]-[7]. Both holes and electrons are the active carriers in conventional PIN-PD. However, because holes have a lower mobility than electrons and because electrical neutrality is imposed by the simple PIN design, the higher mobility electrons acquire a drag inflicted by lower mobility holes.

In photodiodes, there is a trade-off between output power and RF bandwidth. This trade-off is caused by a desire to absorb as much light as possible using thick absorption layers whilst

Maria Jabeen is with the Department of Electronic Engineering School of Engineering, Physical and Mathematical Sciences Royal Holloway, University of London, Egham, Surrey, TW20 0EX, United Kingdom. Contact author, Shyqyri Haxha is with the Department of Electronic Engineering School of Engineering, Physical and Mathematical Sciences Royal Holloway, University of London, Egham, Surrey, TW20 0EX, United Kingdom (email: Shyqyri.Haxha@rhul.ac.uk).

Ian Flint is a visiting professor in the Department of Electronic Engineering School of Engineering, Physical and Mathematical Sciences Royal Holloway, University of London, Egham, Surrey, TW20 0EX, United Kingdom.

Turgut Öztürk and Fathi AbdelMalek were as visiting researchers in Department of Electronic Engineering School of Engineering, Physical and Mathematical Sciences Royal Holloway, University of London, Egham, Surrey, TW20 0EX, United Kingdom. Martin Charlton is the Southampton Nanofabrication Center, University of Southampton, University Road, Southampton, SO17 1BJ, United Kingdom.

separating the electrons and holes rapidly through these thicker layers. Various structures have been tried such as depleted absorbers, hybrid absorbers, partially depleted absorbers, dual absorbers in addition to the combination with UTC-PD [8]-[15]. Hybrid absorbers operate through modifying the trade-off relation between PD efficiency and bandwidth by altering electric field and absorption in absorber regions. The absorption and depletion layers are detached in UTC-PD thereby slightly decouple the optical absorption from the RF bandwidth (speed). In this way the UTC-PD EM field response can be increased whilst maintaining speed [10], [14], [15]. Recently, numerous UTC-PD structures have been proposed including stepped or linear doping in absorption layer, improved heterojunctions, and triple transition region structures [16], [17].

Various layer assemblies of InGaAs/InP UTC-PD have been proposed to Increase the electric field in order to separate the carriers rapidly whilst efficiently absorbing high light intensity. In this way overall performance has been improved [4], [5], [8]. Even InGaAs Schottky barrier photodiodes have been utilised but the barrier height of InGaAs is very low (about 0.2 eV to 0.3 eV) and dark current is very high, and so Schottky barriers are of limited use.

In this paper, a new design of UTC photodiode is proposed using inverted cones and circular dots made of Air voids in absorption and collector layers with the aim to increase electric fields and thereby increase carrier velocity. The idea for this research was an extension of our earlier work on textured layers in solar cells boosting their performance [11], [12]. A Full Vectoral Finite Element Method (FVFEM) has been used through the commercial COMSOL Multiphysics simulation software [18]. This idea is a concept and material growers have not been consulted as to its practicality. The modern fabrication methods are very versatile and the structure appears not too outrageous for manufactures to strive towards the design's performance advantages.

In the next sections, the energy band diagrams of a PIN photodiode and UTC photodiode is illustrated. Then the theoretical analysis behind the modelling of UTC-PD and FVFEM simulation model is given. This will then be compared to a reference benchmark performance of UTC-PD structure [19]. Finally, the new design of UTC-PD with the inverted Air cones and circular dots is optimised by varying the spacer/block layer thicknesses. The final structural configuration delivers increased Electric Field ($\boldsymbol{E}$) in absorber layer of photodiode, improving carrier transportation and higher optical absorption.

The simulation of the photodiode shows electric field distribution through colour representation. The energy band diagram; electron and hole concentration; power loss and power absorbed profile with legends are presented in the next sections.

II. Device Design And Operation

A. Validation

In order to validate the accuracy of our proposed simulation model and structure configuration, we have compared our simulation results with published research in [19]. Similar results were reproduced. The obtained results are presented in the results and discussion section. To make the simulated results comparable, load resistance is set to 50Ω, and width 5um is used. The UTC-PD assembly has a thickness of 1.4μm including contact layers and excluding the light scattering conical texture structure inside absorber and collector region.

B. Epitaxial Structure

Fig. 1 shows the new proposed UTC-PD design. Table 1 lists epi-layer thickness, material type and doping levels. From top to bottom, the proposed layer structure consists of: a 50nm thick very heavily (1×10^{19}) p-doped InGaAs layer provides the top p-contact, followed by a 20nm thick heavily (1×10^{18}) P doped InGaAsP diffusion block layer. A 300 nm thick heavily P-doped InGaAs layer provides the light absorption layer. A 20nm thick undoped InGaAsP diffusion block layer separates the P-N regions, and is followed by a 30nm thick heavily N-doped InP cliff layer. The underlying collector and N-contact layers are lightly (2×10^{16} cm^{-3}) and very heavily n-doped InP layers (thickness 300 nm and 800 nm*)* respectively [20,21].

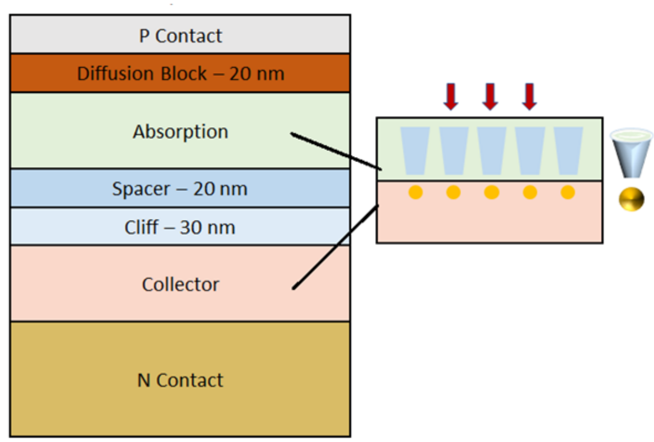

Fig. 1. Schematics of new UTC-PD structure.

The P contact is very heavily doped (1×10^{19} cm^{-3}) but just 50nm thick, whereas the N contact is heavily doped (8×10^{18} cm^{-3}) and very thick (800nm). Since the heavily doped N/P contact layers have no depletion regions they are metallic in nature [22].

This photodiode structure can be grown by epitaxial methods such as Metal - Organic Chemical Vapor Deposition (MOCVD) and Molecular Beam Epitaxy (MBE) [23],[24].

In order to improve the carrier transitions and electric field generation, the following layer properties and doping values were used in Fig. 1 as indicated in Table I and Table II [19].

TABLE I
PROPERTIES OF LAYERS AND MATERIALS FOR PROPOSED UTC-PD CONFIGURATION.

Layers Properties	P Contact	Absorption	Spacer	Cliff	Collector	N Contact
Material	InGaAs	InGaAs	InGaAsP	InP	InP	InP
Thickness (nm)	50	300	20+20	30	300	800
Band Gap (eV)	0.73	0.73	0.88	1.35	1.35	1.35
Doping Level (cm^{-3})	1×10^{19}	1×10^{18}	1×10^{15}	1×10^{18}	2×10^{16}	8×10^{18}
Dopant Type	P	P (N:5×10^{15})	- (N:5×10^{15})	N	N	N
Refractive Index (n)	3.42-3.58	3.42-3.58	3.29	3.2-3.167	3.2-3.167	3.2-3.167
Refractive Index (k)	0.075	0.075	0.0098	0.0	0.0	0.0
Absorption Coefficient (cm^{-1})	10327	10327	941.83	468.72	468.72	468.72
Dielectric Constant	13.8, 12.3	13.8	11.49 10.82	12.5 10.11	12.5 10.11	12.5 10.11
Electron Mobility	12000 cm^2/Vs	12000 cm^2/Vs	5400 cm^2/Vs	5400 cm^2/Vs	5400 cm^2/Vs	5400 cm^2/Vs
Hole Mobility	300 cm^2/Vs	300 cm^2/Vs	200 cm^2/Vs	200 cm^2/Vs	200 cm^2/Vs	200 cm^2/Vs

In this work the addition of inverted cones made of air voids in the absorption layer and circular dots in collector layers play significant role in increasing the electric field and absorption effects. This procedure incorporates air voids through the P-type absorber layer using templated patterning [25,26].
Air voids such as these can be formed by a combination of electron beam lithography, dry etch, and epitaxial overgrowth methods, as has been demonstrated in the recent studies [25,26].

A comprehensive numerical modelling study of the conventional UTC-PD is also provided in recent work [27]. This design of UTC photodiode operates at 1550nm. The bandgap, refractive index and respective material properties are obtained from literature [28],[29] and are also given in Table I and II [19].

C. Electronic Configuration

Under electrically biased illumination conditions, holes generated by light absorption move towards the nearby p-contact, while electrons transit across the depletion region to the collector layer and N-contact.

Since the depletion width in the P region is very small compared to the N region, the p-n junction is said to be one-sided.

In a one-sided junction PIN photodiode, light is normally incident onto the bottom N contact layer and passes over the collector layer, which is often a wide band energy gap material (InP). Then the light is absorbed in the absorption layer region, which is composed of low energy gap material (InGaAs). The electron and hole pairs are produced and separated by the electric field in the absorption layer [30], [31]. In the UTC-PD structure, in contrast, there is a delay time due to the minority electrons crossing over the p-type unbiased absorber side, and the traveling distance is equal to the depletion width. The movement of the minority electrons in direct-bandgap *III–V* materials (for example, InGaAs) is high and quasi-ballistic electron transport appears in the collector, the overall time delay time associated with electron transport can be considerably shortened compared to a PIN structure [30].

TABLE II
MATERIAL PARAMETERS AND PROPERTIES USED IN THE SIMULATION [19]

Parameter	InP	InGaAs
Electron mobility, μ_n	5400 cm^2/Vs	12000 cm^2/Vs
Hole mobility, μ_p	200 cm^2/Vs	300 cm^2/Vs
Conduction band density of states, N_C	5.7×10^{17} cm^{-3}	2.1×10^{17} cm^{-3}
Valence band density of states, N_V	1.1×10^{19} cm^{-3}	7.7×10^{18} cm^{-3}
Electron saturation velocity	2.6×10^{7} cm/s	2.5×10^{7} cm/s
Hole saturation velocity	5×10^{6} cm/s	5×10^{6} cm/s
Electron and hole life time (UTC-PD)	1×10^{-9} s	1×10^{-9} s
Electron and hole life time (OSJ-PD)	2×10^{-9} s	1×10^{-7} s
Electron Auger coefficient	3.7×10^{-31} cm^6/s	3.2×10^{-28} cm^6/s
Hole Auger coefficient	8.7×10^{-30} cm^6/s	3.2×10^{-28} cm^6/s
Real refractive index (1550 nm)	3.165	3.595
Imaginary refractive index (1550 nm)	0	0.075
Bandgap E_g	1.35 eV	0.75 eV
Static dielectric constant ε_r	12.5	13.8
Electron saturation velocity v_e^{sat}	0.85×10^7 cm/s	0.65×10^7 cm/s
Hole saturation velocity v_h^{sat}	-	0.48×10^7 cm/s
Electron mobility μ_e	3500 cm^2/Vs	8000 cm^2/Vs
Hole mobility μ_h	150 cm^2/Vs	300 cm^2/Vs
β	7.4×10^{-13}	7.4×10^{-10}
γ	3	2.5
Electron diffusion coefficient D_e	-	200 cm^2/s
Thermal velocity V_{th}	-	5.5×10^7 cm/s

The electron and hole mobilities, carrier saturation velocities, electron-hole life times and their respective band density states are given in Table 1 and II [19], [30]. In Fig. 2, the electrons (black dots) transit much longer distance through the epi-layers to the contact as compared to the holes (yellow dots) which travel shorter distance to the P-contact. The electron/hole transit time can be adjusted by carefully tuning the electric field across the absorption and collector layers.

COMSOL software based on Full Vectoral Finite Element Method (FVFEM) was used to simulate the epi-layer structure and patterning geometry. This is an additional method using economical commercial software enabling initial assessment novel creative ideas. These ideas might then more formally assessed by basic measurements on the device structures compared to the other software and methods.

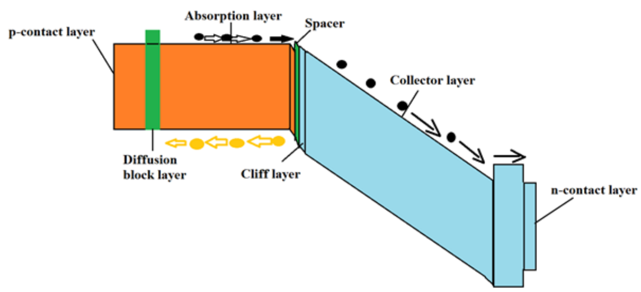

Fig. 2. Simple schematic Energy Band diagram of UTC Photodiode [30]

This alleviates the effort of the designer whilst maintaining the correct physics, such as Electromagnetic wave frequency domain, Electrostatics, Transport of carriers (and dopants) [18],[32],[33]. The software solves Poisson's transport equation, and the continuity equation for electrons and holes [27], [30] [31]. Time average power loss $Q(x, y, z)$ at nodes in the absorber is considered via electric field distribution by using following equations (1)–(6) [19], [27], [30];

$$\nabla^2\psi = -\frac{\rho}{\varepsilon} \tag{1}$$

$$\frac{\partial n}{\partial t} = G_n - R_n + \frac{1}{q}\nabla.\overrightarrow{J_n} \tag{2}$$

$$\frac{\partial p}{\partial t} = G_p - R_p - \frac{1}{q}\nabla.\overrightarrow{J_p} \tag{3}$$

$$\overrightarrow{J_n} = q\mu_n n\vec{E} + qD_n\vec{\nabla}n \tag{4}$$

$$\overrightarrow{J_p} = q\mu_p p\vec{E} - qD_p\vec{\nabla}p \tag{5}$$

$$Q(x,y,z) = \frac{1}{2}c\varepsilon_0\eta\alpha|E(x,y,z)|^2 \tag{6}$$

$$f_{3dB} = \frac{1}{\sqrt{\tau_{tr}^2 + \tau_{RC}^2}} \tag{7}$$

Here ψ denotes the electrostatic potential, ε is the permittivity, ρ is the space charge density, J_n and J_p represents the electron and the hole current densities, μ_n and μ_p are electron and hole mobility, D_n and D_p are electron and hole diffusion coefficients, q is electron charge, G_n and G_p are electron and hole generation rates and R_n and R_p are electron and hole recombination rates. In Equation (6), c is the speed of light, ε_0 is free space permittivity, α is the absorption coefficient (α = 4πk/λ) with k being the imaginary part of complex refractive index, η is the real part of complex refractive index, λ is the wavelength and $\boldsymbol{E}$ *(x, y, z)* is the electric field strength at corresponding excitation wavelength. In equation (7), f_{3dB} represents 3dB bandwidth where τ_{tr} is carrier transition time and τ_{RC} is RC charging time.

The electrical and optical properties of materials used for the simulations including refractive index are taken from literature [27]-[28],[34],[35],[36]. The design parameters and variables are used in the proposed structure simulation are provided in Table 1 and 2. Basic boundary conditions used in the FVFEM simulations are applied to the boundaries/sides of the device and these include: perfect electric conductor, scattering condition, periodic condition, transition boundary condition and surface current density. The model included COMSOL modules of *EM* wave frequency domain, semiconductor model, transport of diluted species, electrostatics, and general Multiphysics compilations. These accounted for the effects of semiconductor optoelectronics interfaces in a simple InP/InGaAs based UTC photodiode structure, and the stimulation of spontaneous emissions in the semiconductor layers. The absorption of the light and the associated change in the electric field distribution are also included in a self-consistent way.

III. Results And Discussions

The electron and hole concentration profiles for reference UTC photodiode and the new proposed UTC PD configuration are illustrated in Fig. 3 and 4. Light is absorbed in the InGaAs absorption region, creating electron hole pairs. The electrons diffuse across the spacer and cliff layers, to the collector layer. A major drawback of this conduction-band offset is space charge build up causes enhanced recombination, leading to a degradation in device bandwidth. Consequently, it is desirable to reduce the effects of the offset.

The high internal electric field is greatly affected by the parameters shown in Table III. Optimisation of these parameters along with the geometrical structures (cones and voids placed in the collector layer) provides a control mechanism. These are fully taken into account in the simulations.

A simple chart in Table III displaying a full investigation of the performance relationship between electric field and other device design parameters, where the upward arrow indicates increasing factor and downward arrow shows decrement. This chart has been designed by taking into account all the simulated parameters to indicate that these parameters have significant effect on Electric field variation. Equation (7) describes the relationship between carrier transit time and 3dB wavelength. We can observe that as the Electric field increase, the 3dB bandwidth of device increases that led to increased carrier transport and decreased Transit time. The output power (OP) of a photodiode can be determined by space charge effect (SCE) and thermal management. The carrier transition time (TS) and charging time can be adjusted independently.

Two optimisations have been applied recently [16],[17]: redesign of spacer layer doping profile, and insertion of a graded layer between absorption and collector layers. Using these two designs approaches the space charge is decreased and the photocurrent loss caused by recombination reduced [16]. Thus, this work presents an approach to utilise modified spacer layer doping profile, a (InGaAsP - 20nm) spacer and cliff layer (InP – 30nm) with suitable doping value of 1 x 10^{15} cm^{-3} and 1 x 10^{18} cm^{-3} was found to be optimal. The blocking photo-generated electrons transitioning from the absorption layer to collector is mitigated.

In Fig. 3 and 4, the electron concentration across the device is shown at different injected light intensities. The electron concentration for reference UTC photodiode structure is also indicated in the inset to Fig. 3 and for holes in Fig. 4. The hole concentration for new design is maximum at the P contact layer and drops down through absorption and collector layer, where the electron concentration increased at the n contact layer (0.8µm to 1µm depth on x-axis frame) and drops at the P contact region for light intensity 1 x 10^4 W/cm^2 to 8 x 10^5 W/cm^2. However, the electron concentration in collector layer stops increasing when light intensity goes above 5 × 10^5 W/cm^2. At these high light levels, a large number of electrons are collected in the absorber layer and saturation occurs. However, for majority carriers, the holes in the heavily doped p-type absorption layer, returns to equilibrium rapidly through the conduction process. As shown in Fig. 3, the hole concentration across the device only varies slightly on changing the light intensities from 1 x 10^4 W/cm^2 to 8 x 10^5 W/cm^2.

TABLE III
RELATIONSHIP BETWEEN ELECTRIC FIELD AND DEVICE DESIGN PARAMETERS

EF ↓	CV ↓	f3-dB BW ↓	Performance ↓	
Doping ↑	EF ↑	ET ↑	f-dB BW ↑	SCE ↓
SCE ↑	EF ↓	f3-dB BW ↓	P_O ↓	
EF ↑	ET ↑	FR ↑	QE ↑	
EF ↑	f3-dB BW ↑	CT ↑	TS ↓	
W_C ↓	EF ↑	TS ↓		
CL	EF ↑	TS ↓	OP ↑	f3-dB BW ↑

EF: Electric Field; BW: Bandwidth; ET: Electron Transport; SCE: Space Charge Effects; P_O: Output Power; FR: Frequency Response; QE: Quantum Efficiency; CT: Carrier Transport (Drift); TS: Transit Time; CV: Carrier (Transit/Drift) Velocity; W_C: Collector Layer Thickness; CL: Cliff Layer; OP: Output Current.

Recently, two significant contactless methods have been utilised practically to limit the semiconductor materials (recombination) lifetime and velocity: the Pump and Probe method (PP) and the Infrared Lifetime Mapping method (ILM), also known as Carriers Density Imaging (CDI) [37]. These methods are used to analyse the free carrier absorption that arises in semiconductor materials. These are based on free carrier absorption contributions present in those material wavelengths with NIR/middle infrared region, corresponding, to the energy lower than the material band-gap. These techniques imply that a distinction of carrier transmittance can be spotted and observed through when a sub-band-gap radiation is transmitted by the material. The PP technique is based on transient methods because they demonstrate a direct analysis to the velocity of the carrier recombination process.

Hence, these are the organized techniques that can be used for this proposed configuration of UTC-PD to determine the concept of carrier recombination lifetime together with the main recombination mechanisms in semiconductor materials.

The key merit to suggest these practical techniques [37] for proposed UTC-PD configuration is the opportunity to directly determine a simultaneous estimation of the bulk recombination carrier lifetime and of the surface recombination velocity.

This slight variation of hole concentration in the absorption to collector layer is primarily due to the light absorbed in the generated inverted cones present in absorption InGaAs layer with 1.1um thickness and small circular nanodots of few nano thicknesses (0.1um) in the collector layer. Similar variations of electron concentration in the absorption to collector layer regions are observed at varying light intensity levels. Therefore, the photo response of a UTC-PD configuration is mainly determined by carrier (electron) transportation.

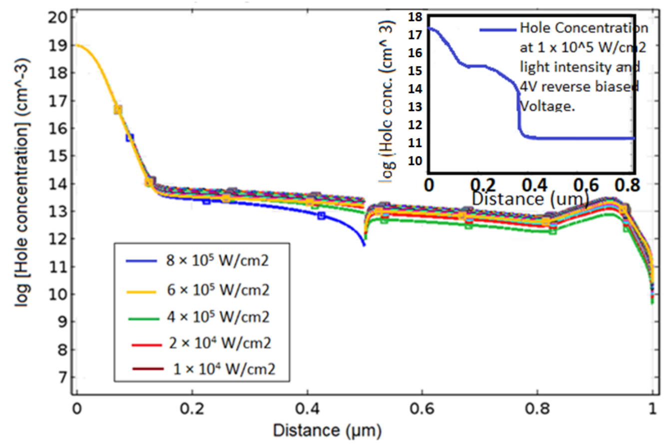

Fig. 3. Hole concentration profiles of proposed UTC-PD structure at different light intensities (different colour lines represent different light intensities starting from 1 × 10^4 W/cm2 to 8 × 10^5 W/cm2). The inset is the reference graph of UTC-PD structure with no textures and plain p-absorption-spacer-collector-n contact layer assembly [19].

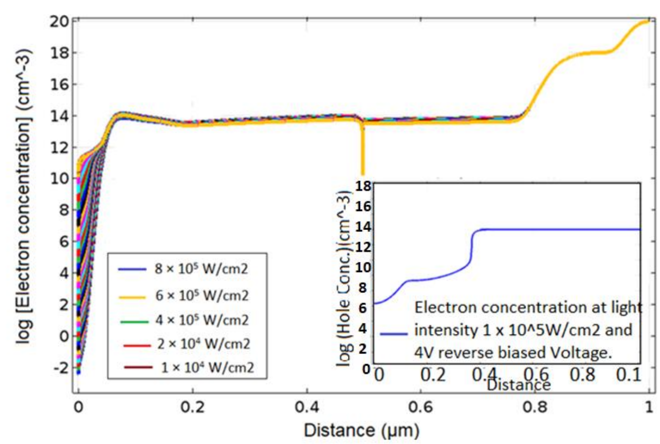

Fig. 4. Electron concentration profiles of proposed UTC-PD structure at different light intensities (different colour lines represent different light intensities starting from 1 × 10^4 W/cm2 to 8 × 10^5 *W/cm2*). Inset Figure is the reference graph of UTC-PD structure with no textures and plain p-absorption-spacer-collector-n contact layer assembly [19].

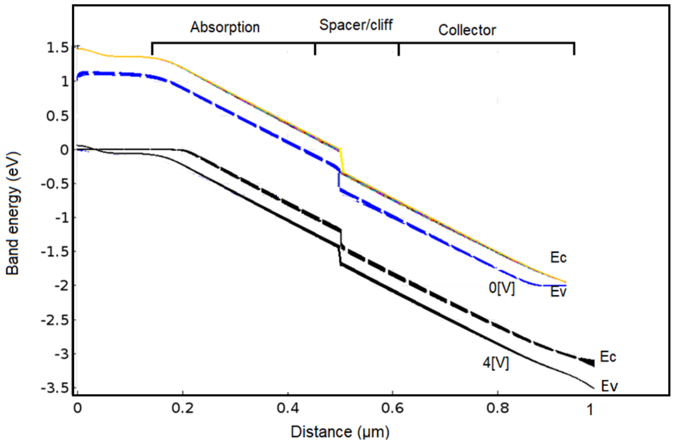

Fig. 5. Simulated energy band diagram of UTC-PD for reverse biased voltage of 0V and 4V.

The electron and hole concentration profiles for UTC photodiode across the device are given in Fig. 3 and Fig. 4, respectively. The band energy diagram for UTC structure for applied voltage of 0V and 4V is presented in Fig. 5. The photogenerated electron-hole pairs are separated by internal generated electric field, and electrons and holes move towards adjacent n-type and p-type contact layers respectively.

The photo response of the proposed photodiode is also simulated, including the carrier concentrations, electric fields and hence velocity of travel. The carrier showed low saturation velocity of 5×10^6 cm/s. Unfortunately, at high light intensities, the electrons in the absorption layer are accumulated, consequently caused the electric field to injected light intensity in the collector, leading to further decreasing their speed. Conversely the hole concentration across the device only varies slightly from low 1×10^4 W/cm^2 to higher light intensities 8×10^5 W/cm^2 as can be seen in Fig. 3. The hole carriers start to gather near the interface between absorption layer and spacer layer at a light intensity of 8×10^5 W/cm^2.

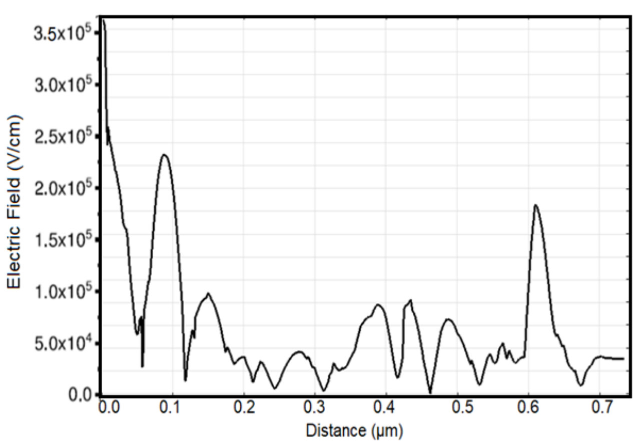

Fig. 6. Simulated internal Electric field of reference UTC-PD structure with 4V reverse biased voltage and with no addition of inverted cones and circular dots in absorption and collector layer.

At high light intensity, not only holes but also electrons tend to collect in this region. This is mainly caused by conduction band cut-off between InGaAs and InP. Due to this carrier build up the internal electric field generation tends to decrease. Once the internal electric field drops to below 40 *kV/cm*, the traveling velocity of holes starts to decrease and holes accumulation occurs. Since there is no valence band discontinuity between p contact layer and absorption layer, the holes can travel easily from absorption layer to the p contact layer.

The energy band diagrams of UTC-PD (Table I) and simulated band energy diagram with reverse biased voltage is illustrated in Fig. 2 and Fig. 5, respectively. The operational mechanism of photodiode structure is given in Fig. 2 [30] where the structure details are described in previous section. In UTC-PD, the electric field in the absorption layer is almost zero. A 20nm thick diffusion block and 30nm thick cliff layers stop photogenerated electrons and holes respectively.

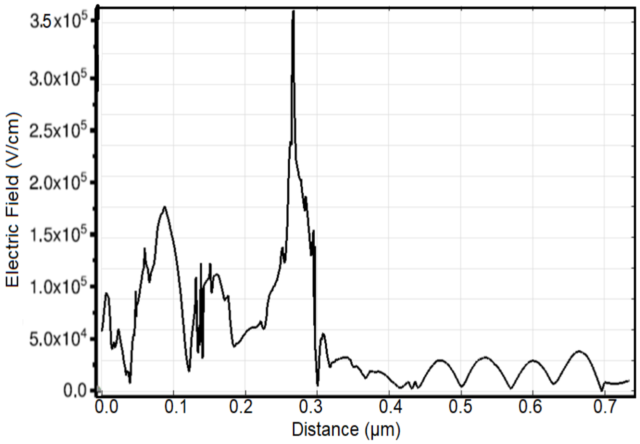

Fig. 7. Simulated internal Electric field of proposed UTC-PD configuration at 10V reverse biased voltage with the addition of inverted cones in absorption layer at incident light intensity 5 x 10^5 W/cm^2.

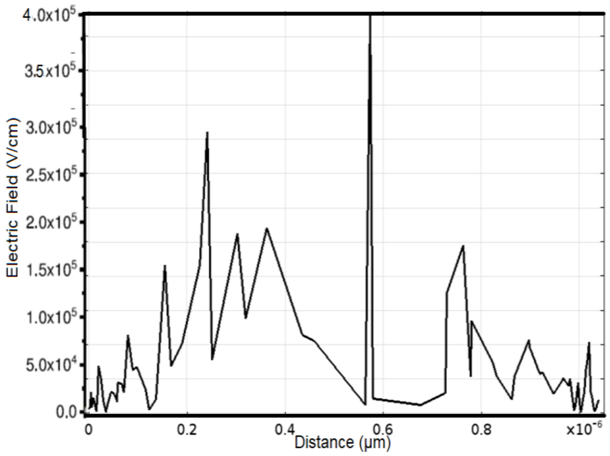

Fig. 8. Simulated Internal field of proposed configuration of UTC-PD at 10V reverse biased voltage with inverted cones and circular dots in absorption and collector layer at incident light intensity of 8 x 10^5 W/cm^2.

The cliff layer increases electric field and facilitate electron transport at the interface between absorption and collector layers. In this simple one-sided junction photodiode structure, the electric field is so high that electrons can travel through spacer layers easily without a cliff layer. The photo-generated electrons in the p-type absorption layer diffuse or drift into the collection layer, while photogenerated holes are swept out as a conduction current within a time of the same order as the dielectric relaxation time. Consequently, only electrons act as the traveling carriers in a uni-travelling carrier photodiode. Speed is limited by transit time of photogenerated electrons across the absorption and collection layers and can be significantly reduced by adjusting the built-in electric field in the absorption layer which can be done by graded-doping along with introduction of nano cones or oval void structures. The light gets multiply scattered by internal cones and this adds to the optical path length and therefore the light absorption efficiency is also increased. Improved light absorption also creates a high internal electric field, as shown in Fig. 7 and Fig. 8.

Obtained internal electric field results for the reference Photodiode structure are shown in Figure 6. The electric field for the unilluminated reference UTC under 4V reverse Bias voltage conditions and with no addition of inverted cones and circular dots in absorption and collector layer can be seen in Fig. 6. Note, the electric field drops to zero at the interface of absorption layer and therefore electrons start to accumulate. The electric field is minimum in the absorption layer and drops throughout the spacer and collector layers.

The electron concentration and electric field in the collector layer for simulated reference PD structure does not increase with higher incident light intensity.

The simulated internal electric field with 10V reverse bias voltage and injected light intensity 5 x 10^5W/cm^2 caused by the addition of inverted cones present in the 1.1um thickness (InGaAs) layer is shown in Fig. 7. The further addition of few 100nm nanodots in the collector layer is shown in Fig. 8. It can be seen that an electric field of magnitude about 3.5 x 10^5 [V/cm] is generated in the absorption region (at x-axis 0.2-0.3 μm) at maximum light intensity 5 x 10^5 W/cm^2. This electric field should be compared to the reference PD structure where the electric field peak is at 5.0 x 10^4 V/cm. Fig. 8 shows the highest internal electric field peak of 4.0 x 10^5 [V/cm] at injected light intensity of 5 x 10^5 W/cm^2 at 10V reverse biased voltage conditions. This field is generated at the transition from the absorption layer to collector layer. This locally high field leads to increased carrier transport and decrease space charge effects. Notably, the reverse bias voltage has a great influence on the electric field accumulation/ space charge effect, and photocurrent. Photocurrent density usually because the carriers normally self-screen and not rapidly separated by the field. Thus, it is essential to decrease the offset in conduction band. Electric and magnetic field distributions of the proposed structure are illustrated in Fig. 9 where three different thickness (A,B,C) of internal layer assemblies have been simulated. From these figures field distributions in the internal structure of the diode can be seen.

In the above simulated PD, a uniform doping profile in absorber along with enhanced inner photon scattering is employed. A built-in electric field was generated in the absorption layer by introducing light scattering textures (as shown in Fig. 9) along with layer doping profiles as shown in Table 1. The inverted light scattering cones made of Air voids have a period of between 0.2 um and 2 um. Inverted cones in the absorption (InGaAs) layer with 1.1 um height and small circular nanodots of diameter (0.1um) is integrated. The periodicity in the collector layer is 0.3um in this UTC PD configuration.

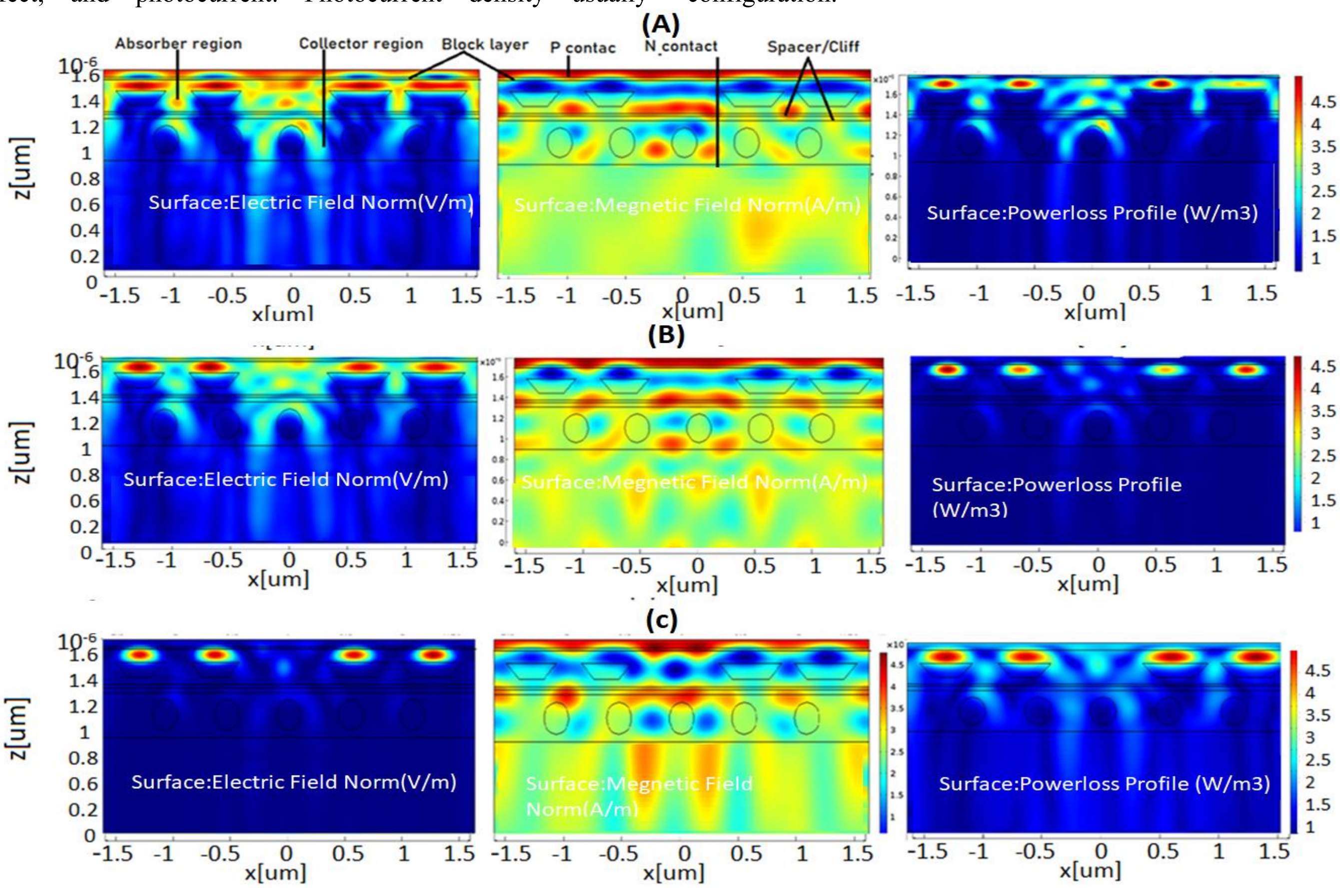

Fig. 9. Electric field distribution, magnetic field distribution and power-loss profile in UTC PD configuration under frequency conditions 2.7259E14m and high light intensity 6 x 10^5 *W/cm2*, where the red colour in colour legends represent highest magnitude of ***EM*** field and blue color represent minimum levels of field. (A) The thickness of Block layer-10 *nm*, Spacer layer-10 *nm*, Cliff layer 20 *nm*. (B) The thickness of Block layer- 15 *nm*, Spacer layer-15 *nm*, Cliff layer-25 *nm*. (C) The thickness of diffusion block layer-20 *nm*, Spacer layer-20 *nm*, Cliff layer-30 *nm*

increases with bias voltage. It is worth mentioning that the space charge effect in UTC-PD can be relaxed by modifying uni-traveling carrier photodiode structure.

The conduction-band step between InP and InGaAs can be used to unblock the movement of carriers to the collection layer and thereby prevent their accumulation in the absorption layer. This decrease space charge increases bandwidth

It is observed that by increasing of the thickness of both blocking layer and spacer layer, the electric field near the output side of the absorber layer is increased and the electric field in the collector layer drops away, as shown in Fig. 9 (A, B, C). As, the thickness of blocking layer and spacer layer increases from 10nm to 20nm, the electric field near the output side of the absorber region and the electric field in the collector region increases and decreases, respectively. It can be seen in Fig. 9 (C), the electric field and power loss profile of the device changes more rapidly with a 10nm change in thickness of the spacer layer to 20nm and cliff layer thickness of 30nm than when the spacer layer of thickness 10 *nm* and cliff layer 20nm (Fig. 9(A)). This is due to the fact that the junction capacitance and the electric field of the UTC-PD device is more sensitive to the change of the parameters of spacer/block layers, as shown in Fig. 9.

It is well known that the greatest effect of surface recombination exists for materials with known low surface recombination, such as InGaAs, which has a thin layer relative to its diffusion constant. Similarly, increased recombination occurs when the intensity of light shifts the number of carriers away from equilibrium.

A recent publication proposes a method of passivation of InGaAs columns/pillars (possibly similar to the absorption layer in proposed UTC-PD structure) uses a method to measure the improvement factors [38]. Thus, the published fabricated device has presented the ALD (Atomic Layer Deposition) method for passivation and measured the effects to get comparable results. The manufacturing of the micro/nanopillars was performed using Electron Beam Lithography (EBL) and dry etching processes and the surface passivation treatment comprised a mild wet etching of the active material in an ammonium sulfide, $(NH_4)_2S$, chemical solution followed by Silicon Oxide, SiO_2, encapsulation by Plasma-Enhanced Chemical Vapor Deposition (PECVD) [38]. This recently published method using InGaAs/InP nanopillars, (with a re-producible, strong, and long-standing passivated surface) can be benchmarked to pre-test and fabricate the nano cones and dots in the proposed UTC-PD layer arrangement.

This method can be used to pre-test the proposed photodiode layers before manufacturing of complete UTC-PD device.

Air voids such as these can be created by a combination of electron beam lithography, dry etch, and epitaxial overgrowth methods, as has been demonstrated in the recent studies [25,26].

In Fig. 9, it can be observed that, the average electric-field strength in the absorber layer and collector layer is increased and decreased, respectively, by varying the thicknesses of spacer layers under light intensity 6 x10^5W/cm^2. The increased electric field strength in entire region is presented by colour legends. Here, the red and yellow dots represent the maximum generated ***EM*** field effects (electric field in *V/m*, magnetic field in *A/m*) and accordingly the power loss profile (amount of power absorbed in the absorber layer) is presented by unit W/m^3. It is observed that the electric field strength in the absorption layer (the circular red coloured fringes) and collection layer (blue domain) is enhanced to a certain degree by increasing the period of 2 sets of inverted cones placed near the blocking layer side (diffusion block layer-20nm), as shown in Fig. 9.

The conduction band offset and valence band offset increase and decreases, respectively, when the p doping concentration is different between absorption layer and electron barrier layer. This can result in an improved barrier to prevent the diffusion of photogenerated electrons from the absorption layer to the p-contact layer. Meanwhile, such doping enables the photogenerated holes to better reach the p-contact layer. From Fig. 9, it can be seen that the electric-field distribution in the device is more sensitive to the integrated circular dots and inverted cones in the absorption layer and collector layer as well as the thickness of spacer layers.

From the optimisation of the proposed structure, the output power loss profile (*W/m³*) of the UTC-PD is improved and more light is captured in the active region. Under high light intensity the photogenerated electrons drift more easily into the collection layer with proposed structure, accordingly increasing the bandwidth of the device.

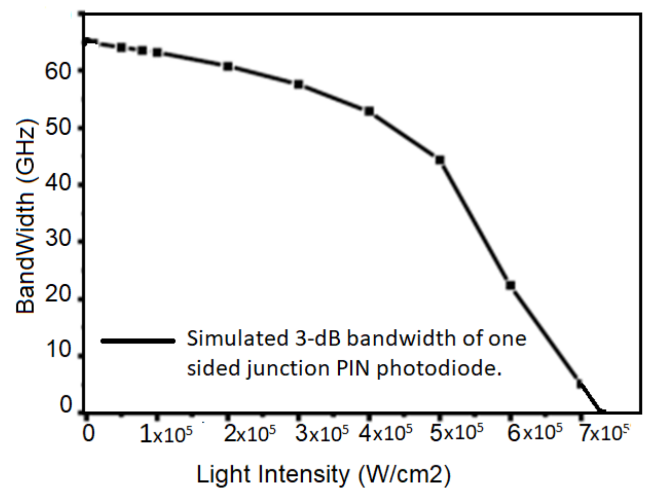

Fig. 10. Simulations of Bandwidth versus Light intensity for One sided Junction PIN photodiode.

High intensity light causes high concentrations photo-generated electrons and it will lead to decrease the depleted region and the loss of the electric field. Nevertheless, the potential spike becomes larger and the energy band becomes flat.

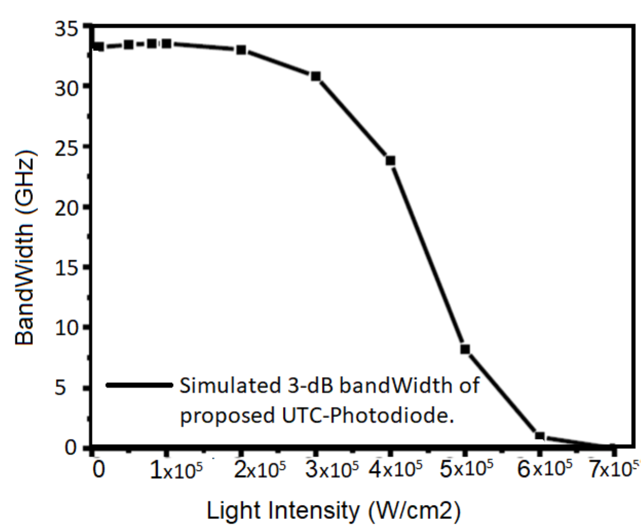

Fig. 11. Simulations of Bandwidth versus Light intensity for

improved Uni travelling carrier photodiode.

In the simulated UTC photodiode structure, the thickness and doping levels of diffusion block layer, spacer and cliff layer have significant influence on electric field distribution of UTC-PD, as can be seen in Fig. 9.

The bandwidth responses of UTC photodiode and one-sided junction basic photodiode structures are simulated and obtained as shown in Figs. 10 and 11. As a comparison, for both structures, the bandwidth drops because of space charge effect gradually when light intensity increases. Their mechanisms for bandwidth variation spectrum are different. For UTCPD, electrons are driven by concentration rise in the absorption layer. As shown in Fig. 4, electron concentration rise is noticeable when light intensity is below 4×10^5 W/cm^2 and the gradient varies at light intensities above 5×10^5 W/cm^2. The distinction of electron concentration incline in Fig. 4 approves the gradient variation of bandwidth in Fig. 11. In case of one-sided photodiode, both electrons and holes are affected by inner electric field. As can be seen in Fig. 10, the internal electric field decrease to zero at high light intensity of 7×10^5 W/cm2. The internal electric field variation in Fig. 6,7 agrees well with the simulation graph of bandwidth in Fig. 10,11. As shown in Figs. 10 and 11, the UTC-PD with 300 nm absorption layer and collector layer has a bandwidth of 34 GHz at low light intensity, while the one sided junction PD bandwidth has a bandwidth of 65 GHz at low light intensity.

In this study, it is observed that with the specific thicknesses of the spacer layer the electric field is strongly confined in absorber regions and become more prominent in those active layers. Thus, from the *EM* field distribution in the proposed configuration can be observed that the photo-generated carriers can simply travel to the contact layers where they can be collected. The built-in electric field dispersal appears uniformly from top to bottom of the device and tends to increase the output efficiency by increasing the concentration of active carriers.

IV. Conclusion

A new structure configuration of InP/InGaAs based UTC-PD is designed, analysed and optimised using FVFEM. The concept of UTC-PD is different from the one sided-PD in the epitaxial layer structure, internal electric field distribution, energy band diagram and operation mechanism. The proposed UTC-PD structure with 300 nm absorption layer thickness has achieved a bandwidth of 65 GHz and highest internal electric field peak of 4.0 x 10^5 [V/cm] under 10V bias voltage. It has been demonstrated that the proposed configuration exhibits major performance characteristics such as; increased electric field for improved speed; increased optical scatter for improved transport of electrons and holes to promote high power handling. The key design performance parameters are optimised enabling the reduction of electron and hole concentration self-screening; electric field distribution (1D and 2D) whereas the thicknesses and materials of block/spacer layers are adjusted to enhance the semiconductor physics. The entire structure is simulated through Finite Element Method (FEM) using commercial software. The proposed design is verified for fabrication application through recent benchmarked practical techniques (such as Electron Beam Lithography (EBL), dry etching processes and the surface passivation treatment) and would have significant benefits photodetectors for ultra-high-speed state-of-the-art fibre-optic communication systems, and THz generation with high output power there by help fill the THz gap.

References

[1]. A. J. Seeds, and K.J. Williams, ‘’Microwave photonics’’, *Journal of Lightwave Technology’’*, vol. *24*, no. 12, pp. 4628-4641, 2006.
[2]. J. W. Shi, C. Bin Huang, and C. L. Pan, “Millimeter-wave photonic wireless links for very high data rate communication,” *NPG Asia Mater.*, vol. 3, no. 4, pp. 41–48, 2011.
[3]. T. Ishibashi, N. Shimizu, S. Kodama, H. Ito, T. Nagatsuma, T. Furuta, ‘’Uni-travellingcarrier photodiodes in: Tech. Dig. Ultrafast Electron’’. *Optoelectron, paper UC3*, pp. 166–168, 1997
[4]. Ito, H., Kodama, S., Muramoto, Y., Furuta, T., Nagatsuma, T. and Ishibashi, ‘’High-speed and high-output InP-InGaAs unitraveling-carrier photodiodes’’. *IEEE Journal of selected topics in quantum electronics*, vol. 10*,* no. 4, pp. 709-727, 2004.
[5]. T., R.S., Taylor, A.J., Burrus, C.A., Eisenstein, G. and Wiesenfeld, J.M, ‘’Coaxially mounted 67 GHz bandwidth InGaAs PIN photodiode’’. *Electronics Letters*, vol. 22, no. 17, pp. 917-918, 1986.
[6]. D.G. Parker, ‘’The theory, fabrication and assessment of ultra-high-speed photodiodes’’, *GEC journal of research*, vol. 6, no, 2, pp. 106-117, 1988.
[7]. K. Kato, S. Hata, K. Kawano, and A. Kozen, ‘’Design of ultrawide-band, high-sensitivity pin photodetectors’’. *IEICE Transactions on Electronics*, vol. 76*,* no. 2, pp. 214-221, 1993.
[8]. Y. Muramoto, and T. Ishibashi, ‘’InP/InGaAs pin photodiode structure maximising bandwidth and efficiency’’, *Electronics Letters*, vol. 39*,* no. 24, pp.1749-1750, 2003.
[9]. Li, X., Demiguel, S., Li, N., Campbell, J.C., Tulchinsky, D.L. and Williams, K.J, ‘’Backside illuminated high saturation current partially depleted absorber photodetectors’’, *Electronics letters*, vol. 39*,* no. 20, pp.1466-1467, 2003.
[10]. J. W. Shi, Y. S. Wu, C.Y. Wu, Chiu, P.H. and C. C. Hong, ‘’High-speed, high-responsivity, and high-power performance of near-ballistic uni-traveling-carrier photodiode at 1.55-µm wavelength’’. *IEEE photonics technology letters*, vol. 17*,* no. 9, pp. 1929-1931, 2005.
[11]. M. Jabeen, S. Haxha, S. member IEEE, and M. B. . Charlton, “Improved Efficiency of Microcrystalline Silicon Thin-Film Solar Cells With Wide Bandgap CdS Buffer Layer*,” IEEE Photonics J.*, vol. 9, no. 6, 2017.
[12]. M. Jabeen, and S. Haxha, ‘’High rear reflectance and light-trapping in textured graphene-based silicon thin-film solar cells with back dielectric-metal reflectors’’. *OSA Continuum*, vol. 2, no. 5, pp. 1807-1821, 2019.
[13]. E. Rouvalis, C. Renaud, C., Moodie, D.G., Robertson, M.J. and Seeds, A.J, ‘’Traveling-wave uni-traveling carrier photodiodes for continuous wave THz generation’’. *Optics Express*, vol. 18*,* no. 11, pp.11105-11110, 2010.
[14]. T. Ishibashi, Y. Muramoto, T. Yoshimatsu, and H. Ito,. ‘’Unitraveling-carrier photodiodes for terahertz applications’’, *IEEE Journal of Selected Topics in Quantum Electronics*, vol. 20*,* no. 6, pp. 79-88, 2014.
[15]. G. Zhou, P. Runge,S. Keyvaninia, S. Seifert, W. Ebert, S. Mutschall, A. Seeger, Li, Q. and A. Beling, ‘’High-power InP-based waveguide integrated modified uni-traveling-carrier photodiodes’’. *Journal of Lightwave Technology*, vol. 35*,* no. 4, pp. 717-721, 2017.
[16]. J. Xu, X. Zhang, and A. Kishk, ‘’Design of modified InGaAs/InP one-sided junction photodiodes with improved response at high light intensity’’. *Applied optics*, vol. 57*,* no. 31, pp. 9365-9374, 2018.
[17]. M. Chtioui, D. Carpentier, S. Bernard, B. Rousseau, F. Lelarge, F. Pommereau, C. Jany, A. Enard, and M. Achouche, ‘’Thick

absorption layer uni-traveling-carrier photodiodes with high responsivity, high speed, and high saturation power''. *IEEE Photonics Technology Letters*, vol. 21*,* no*.* 7, pp. 429-431, 2009.

[18]. W. B. Zimmerman, ''Multiphysics modelling with finite element methods'', *World Scientific Publishing Company* , vol. 18, 2006.

[19]. J. Xu, X. Zhang, and A. Kishk, ''Design of high speed InGaAs/InP one-sided junction photodiodes with low junction capacitance''. *Optics Communications*, vol. 437, pp. 321-329, 2019.

[20]. Okamoto, A. and Ohata, K., 'Selective epitaxial growth of gallium arsenide by molecular beam epitaxy'. *Applied physics letters*, vol. *51, no.* 19, pp.1512-1514, 1987.

[21]. Yarn, K.F., Chien, W.C., Lin, C.L. and Liao, C.I., 'Direct growth of high-quality InP layers on GaAs by MOCVD'. Active and passive electronic components, vol. 26, no. 2, pp.71-79, 2003

[22]. C. Hu, ''Modern semiconductor devices for integrated circuits'' vol. 2, 2010.

[23]. X. Lin, M. Natrella, J. Seddon, C. Graham, C. Renaud, M. Tang, J. Wu, H. Liu, and A.J. Seeds, ''High performance waveguide uni-travelling carrier photodiode grown by solid source molecular beam epitaxy''. *Optics express*, vol. 27*,* no*.* 25, pp. 37065-37086, 2019.

[24]. M. Natrella, E. Rouvalis, C.P. Liu, H. Liu, C.C. Renaud, and Seeds, A.J, ''InGaAsP-based uni-travelling carrier photodiode structure grown by solid source molecular beam epitaxy''. *Optics express*, vol. 20*,* no*.* 17, pp. 19279-19288, 2012.

[25]. Liu, J.Z., Charlton, M.D., Lin, C.H., Lee, K.Y., Krishnan, C. and Wu, M.C., 'Efficiency improvement of blue LEDs using a GaN burried air void photonic crystal with high air filling fraction'. *IEEE Journal of Quantum Electronics*, vol. *50, no.* 5, pp.314-320, 2014.

[26]. Tsai, Y.L., Liu, C.Y., Krishnan, C., Lin, D.W., Chu, Y.C., Chen, T.P., Shen, T.L., Kao, T.S., Charlton, M.D., Yu, P. and Lin, C.C. 'Bridging the "green gap" of LEDs: giant light output enhancement and directional control of LEDs via embedded nano-void photonic crystals. Nanoscale, vol. 8, no. 2, pp.1192-1199, 2016

[27]. S. Srivastava, and K.P. Roenker, ''Numerical modeling study of the InP/InGaAs uni-travelling carrier photodiode'' *Solid-State Electronics*, vol. 48*,* no. 3, pp. 461-470, 2004.

[28]. E. Palik, ''Handbook of Optical Constants of Solids'', vol. 1. (*Academic*, 1998).

[29]. M. Polyanskiy. Database Refractive Index. Accessed: Sep. 14, 2015. [Online]. Available: http://refractiveindex.info.

[30]. T. Ishibashi, and H. Ito,''Uni-traveling-carrier photodiodes'', *Journal of Applied Physics*, vol. *127, no.* 3, pp. 031101, 2020.

[31]. T. Ishibashi, T. Furuta, H. Fushimi, S. Kodama , H. Ito, T. Nagatsuma,N. Shimizu, and Y. Miyamoto, ''InP/InGaAs uni-traveling-carrier photodiodes''. *IEICE transactions on electronics,* vol. 83*,* no. 6, pp. 938-949, 2010.

[32]. M. Hamady, E. Kamrani, and M. Sawan, ''Modeling cmos pin photodiode using comsol.'' *In 2012 24th IEEE International Conference on Microelectronics (ICM),* pp. 1-4, 2012.

[33]. R.W. Pryor, ''Modeling PIN Photodiodes'', *COMSOL conference, Boston, USA, 2010*.

[34]. S. Adachi, and Tu, C.W., ''Physical Properties of III-V Semiconductor Compounds: InP, InAs, GaAs, GaP, InGaAs and lnGaAsP.'' *Physics Today*, vol. 47*,* no*.* 2, p.99, 1994.

[35]. S. Srivastava, ''Simulation study of InP-based uni-traveling carrier photodiode ''(Doctoral dissertation, University of Cincinnati), 2003

[36]. ''New semiconductor materials, characteristics and properties'', http://www.ioffe.rssi.ru/SVA/NSM/. (Accessed February 2018).

[37]. De Laurentis, M. and Irace, A., 2014. Optical measurement techniques of recombination lifetime based on the free carriers absorption effect. Journal of solid state physics, 2014.

[38]. Higuera-Rodriguez, A., Romeira, B., Birindelli, S., Black, L.E., Smalbrugge, E., Van Veldhoven, P.J., Kessels, W.M.M., Smit, M.K. and Fiore, A., 2017. Ultralow surface recombination velocity in passivated InGaAs/InP nanopillars. Nano letters, 17(4), pp.2627-2633.

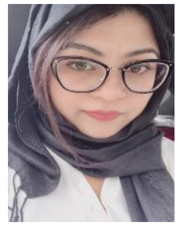

Maria Jabeen received the MSc degree in Physics from GCUF Pakistan, in 2013 and the MSc degree in Electronic Engineering from University of Bedfordshire, UK, in 2015. She received the Ph.D. degree in Electronic Engineering (Renewable Energy Modelling) from Royal Holloway University of London, UK, in 2020. Her research interest includes the Silicon solar cell modelling, new generation materials including graphene/graphite, Physics engineering, development of novel solar cell structures exhibiting high absorption efficiency, nanophononics and physics including fields nuclear atomic physics, quantum mechanics, solid state and plasma physics and electrostatics, Surface texturing, and multijunction layers with 2D/3D techniques using FVFEM, fundamental study of thin-film solar cells of nanostructured surfaces.

Shyqyri Haxha (SM'14) received the MSc and PhD degrees from City University in London in 2000 and 2004, respectively. He has also obtained several world-class industrial trainings and diplomas such as Executive MBA Cambridge Judge Business School and Mini Telecom MBAs. He was awarded the SIM Postgraduate Award from The Worshipful Company of Scientific Instrument Makers in Cambridge for his highly successful contribution in research. Currently, he is a Reader at Royal Holloway, University of London, Department of Electronic Engineering Egham, Surrey, United Kingdom. He was also a Reader in Photonics in the Computer Science and Technology, University of Bedfordshire, Luton in the United Kingdom. Prior to these posts, he was a lecturer in Optic Communication at the School of Engineering and Digital Arts, University of Kent, Canterbury, United Kingdom. Dr Haxha expertise is focused on designing and optimizing, photonic and microwave devices, and systems for applications in Sensor Technology (Medical and Environmental), Nanotechnology and Telecommunication Systems. Dr Haxha research interests are in the areas of microwave photonics, photonic crystal devices, metamaterials, photonic crystal fibers, nano-sensors, optical sensors, surface plasmon polaritons (SPP), biosensors, ultra-high-speed electro-optic modulators, compact integrated optic devices, Optical CDMA, Optical FDM, and Optical MIMO systems. He has developed and demonstrated RF over fiber transmission systems for the aviation industry, including cybersecurity protection for commercial and defense applications. He is a Chartered Engineer (CEng), Senior Member of the Institution of Electrical and Electronics Engineers (Senior MIEEE), Fellow of the Higher Education Academy (FHEA), Editorial Board Member for MDPI journals and Associate Editor of IEEE Sensors Journal. He has been a keynote speaker of numerous world class conferences.

Ian Flint received his BSc in Physics with Maths from Reading University, in 1975. In 1982, he received his PhD from Reading University on "The electron spin resonance of low temperature irradiated diamond". Prof. Ian Flint is a visiting Professor at Royal Holloway University London. He was the first to identify the role of self-interstitials to enhanced diffusion of impurities. He is a physicist, previously working for 10 years in the Universities of Reading (1978 year to 1982), Hull University (from 1982 to 1983) Oxford University (1983 to 1985) Bath University (1985 to 1989) and on optoelectronics and Solid-State physics. In 2004 Prof. Flint received BAE Systems Chairman's Gold individual award for a photonic microwave filter design. Prof. Flint is inventor of Seventeen filled patents for three different companies in the last 20 years. He has a wide range research expertise and development roles in university and industry. Initially working in solid state physics and then integrated photonics. On moving to industry his work allowed first commercially back-illuminated CCD devices. These back-illuminated processes allowed major systems like the Hubble space telescope (the current WFC3 devices). These devices are sixteen times more sensitive in the blue and UV wavelength than the previous device. He is the inventor of large number of patent filing awards within Marconi Optical Components, Selex (Leonardo). Marconi, E2V, BAE systems. Patents are filed in RF sampling and RF down conversion, Laser Hybridisation; Laser machined waveguides; Integrated Optical Isolators Micro Mechanical devices; Blowing fibre into coil winding; Monitoring surface properties; In situ waveguide deposition; Microwave photonic filters; Multi Input receiver, RF Sampling; Simulated Brillouin Scattering, Imaging Devices and Systems etc.

Dr. Ozturk received his M.Sc. and Ph.D. degrees in Electrical and Electronics Engineering from the Karabuk University in 2013 and 2016, respectively. He is currently working as an Associate Professor at Bursa Technical University from 2016 and besides, he was a researcher at Millimeter and Terahertz Technologies Research Laboratories (MILTAL) in TUBITAK-MRC until 2018. His current research is focused on THz radiation, microwave-THz spectroscopy systems, electromagnetic material characterization, and detection of explosive and illicit liquids and design of detector/sensor for THz applications.

Martin D.B. Charlton is professor of nano-photonics, and nano-fabrication at the at the University of Southampton UK. He held a ‘Royal Society Research Fellowship’ for 10 years, was awarded the “Rank phd thesis prize” in 1999, and founded Mesophotonics ltd in 2001. His research interests include: Diffractive Optics, directional VCSELs and LEDs, Hybrid LEDs and Photovoltaics and Micro-Displays. He holds 33 granted patents in the field of photonic quasi-crystals, has over 200 academic publications and holds visiting Professor positions at JAIST (Japan) and Xian Jiatong University (China).

Fathi AbdelMalek received the MSc and PhD degrees from Institut des Sciences Appliquées et de Technologie and Ecole Centrale de Lyon, France, in 1996 and 1999, respectively. He had developed models and numerical schemes in nanoscales structures combining photon-electron along with experimental measurements in femtosecond lasers, photonic integrated devices and sensors. He was a Research Associate and a Research Fellow at U.S. and U.K. universities, where he carried out research on ultrafast photonics, nanophotonic for applications in telecommunication and aerospace technology, metalenses, and biosensors for use in medicine and environment industry. He was awarded several Awards for his contribution in research. Currently, his interest is designing and developing new generation of nanobiosensors for applications in health care (early detection of diseases such as identifying viruses, studying cancer cells early detection, brain tumours, drug delivery), also, using quantum nanophotonic and artificial intelligence for the design of integrated optical smart systems for applications in renewable energy and medical fields.